

Multi-metal contamination of a calcic cambisol by fallout from a lead-recycling plant

M. Cecchi^a, C. Dumat^a, A. Alric^a, B. Felix-Faure^b, P. Pradere^c, M. Guiresse^{a,*}

^a Laboratoire EcoLab. UMR. 5245 (CNRS-INP-ENSAT-UPS), 1 Av de l'Agrobiopole, BP 32607 Auzeville-Tolosane, 31326 Castanet-Tolosan, France

^b Lara Europe Analyses 1 impasse de Lisieux, B.P. 82553, 31025 Toulouse Cedex 3, France

^c STCM 11 route de Pithiviers, 45480 Bazoches-les-Gallérandes, France

Received 2 May 2007; received in revised form 22 October 2007; accepted 28 November 2007

Available online 18 January 2008

Abstract

The present study deals with the impact of a lead-recycling plant on metal accumulation in soils, evaluated by a global pedological analysis. This general approach can be used on various contaminated sites to evaluate impact of an anthropogenic activity and inform on metal origin and behavior. A soil profile collected in the vicinity of a lead-recycling plant in operation for 40 years was studied. Correlations between major and trace elements highlighted different patterns of metals according to their origins. Two groups of metals were identified: (i) Pb, Sb, Sn, As, Cu and Zn of anthropogenic origin and (ii) Ni and Cr of natural origin. The results showed that Pb, Sb and Sn presented the highest relative contamination followed by Cu, As and Zn. Moreover, Pb and Sb migrated most along the profile at an estimated rate of 1.5 cm y^{-1} , followed by Sn, then Zn, Cu and finally As. Sequential extractions showed that all metals were mainly solubilized by reduction and therefore estimated to be bound to iron oxides, except lead which was rather in the acid-soluble fraction in the contaminated horizons. Furthermore, high levels of lead were found in water-soluble and exchangeable fractions (4.2 mg kg^{-1}) suggesting the occurrence of lead transfer towards the trophic chain.

Keywords: Trace elements distribution; Sequential extraction; Soil profile; Metal binding minerals; Risk assessment

1. Introduction and context

Lead is a potentially toxic metal that occurs naturally in soils (its natural occurrence is related to the composition of the bedrock), in concentrations ranging from 1 to $200 \text{ mg Pb kg}^{-1}$ soil with a mean of 15 mg kg^{-1} (Alloway, 1995; Baize, 2002). Lead can also enter the soil through numerous anthropogenic activities: the metallurgical industry, mining and smelting, electroplating, vehicle exhaust, energy and fuel production, soil fertilization and pesticide applications (Dumat et al., 2001; Alkorta et al., 2004). Indeed, lead owes the development of its uses to its physico-chemical characteristics (low melting point, resistance to acids and corrosion, absorption of radiation). Due to its persistence and numerous uses, lead is therefore one of the most common pollutants in the environment. It can enter the human food chain

via contaminated meat or water, crops grown on contaminated soils and also direct incidental ingestion of contaminated soil particles by young children (Alloway, 1995). This poses a major environmental problem because lead uptake can cause negative effects on human health like irreversible disorders of the nervous, digestive and reproductive systems, or anaemias (Ahmed and Siddiqui, 2007). Indeed, lead is potentially toxic to many living organisms even at low concentrations. Risk to humans occurs at above $400\text{--}500 \text{ mg Pb kg}^{-1}$ soil (US EPA, 2001). That is why lead is a major focus for research.

Although the utilizations of lead are becoming increasingly limited, its electrochemical properties make it highly suitable for manufacturing batteries, which is one of the main current uses of lead. Indeed, batteries represent 70% of the raw material for the recycling of lead, 160 000 t being treated in France per annum. The recycling process is carried out in several stages (crushing, fusion, reduction and refining), each generating undesirable by-products such as Cu, Zn, As, Sb, Sn, Bi and Ag. This is why soils close to this kind of plant could present multi-metal contamination.

* Corresponding author. Tel.: +33 5 62 19 39 37; fax: +33 5 62 19 39 01.
E-mail address: guiresse@ensat.fr (M. Guiresse).

The first objective of the present study was therefore to assess the global impact on soil of lead-recycling plants, essential in today's industrial context. To do so, a global pedological approach was used to assess the behavior of lead and other metals generated by the process, but also their speeds of migration. Many studies have already been conducted on surface polluted soils located in urban environments (Chirenje et al., 2004; Banat et al., 2005; Elless et al., 2007). But, only few deal with the behavior of lead along the soil profiles in the industrial setting of atmospheric fallout (Dumat et al., 2001). Indeed, the literature generally reports that lead accumulates in the surface soil horizon because of its low mobility and strong association to soil constituents. In the case of non-point source pollution, endogenous and exogenous lead can be assessed by determination of the isotopic ratio. Such analyses are very expensive and not necessary in the case of point source pollution, with very high abnormal lead concentrations in soils surrounding the pollution sources.

Our work is based on a calcic cambisol profile (FAO, 1998) collected within the grounds of a lead-recycling plant which has been in operation since 1967 in Bazoches-les-Gallérandes (45, France). The global pedological approach first consisted in the determination of the pedo-physical-chemical characteristics (pH, cationic exchange capacity, organic matter, carbonates and phosphorus contents) and then of the metal concentrations along the soil profile. The relationship between trace and major elements was completed by additional measurements like direct observation with SEM and chemical extractions.

The last objective was to estimate the availability and distribution of trace elements along the profile. Indeed, metals can interact with the soil constituents and thus exist in various solid phase fractions, which govern their mobility and bioavailability (Dumat et al., 1997, 2001). This distribution can be measured by selective sequential extraction (Tessier et al., 1979), based on the solubility of individual solid phase components by selective reagents (Han et al., 2003). A large number of sequential extraction procedures have been developed (Tessier et al., 1979; Ure et al., 1995; Quevauviller et al., 1996). They have been criticized: a lack of specificity of the reagents and reported problems with metal redistributions and readsorption during the extraction procedure have been seen as drawbacks to the procedure (Raksasataya et al., 1996; Schramel et al., 2000). But, some studies, showed that the degree of readsorption was less than expected and that it did not invalidate the sequential extraction results (Ho and Evans, 2000; Bacon et al., 2006). This study, concerning a calcareous contaminated soil, used a sequential chemical extraction procedure, as reported by Leleyter and Probst (1998), which has a specific step to determine the carbonate fraction.

2. Materials and methods

2.1. Pedological analyses

The global pedological analysis developed in this study began by the determination of soil characteristics along a profile sampled every 10 cm. The soil pH was measured in water using a 1:2.5 soil/solution ratio according to the standard ISO 10390 procedure. After removal of organic matter with H_2O_2 and soil dispersion

with sodium hexametaphosphate, granulometric analysis was carried out by sieving (for sand), sedimentation and extraction with a Robinson pipette (for clay and silt). The size fractions obtained were then classified as clay ($<2 \mu\text{m}$), silt ($2\text{--}50 \mu\text{m}$) and sand ($50\text{--}2000 \mu\text{m}$). The cationic exchange capacity (CEC) was obtained by the Metson method (1 mol L^{-1} ammonium acetate, pH 7 and 1 mol L^{-1} NaCl). For determination of CaCO_3 , CO_2 released by addition of HCl was measured with a calcimeter. Available phosphorus was assayed with the Joret–Hebert method. Organic carbon was measured using the wet oxidation method. As the availability of metals is influenced by active minerals like clay, that present numerous adsorption sites for metals, clay mineralogy was obtained after dispersion (successive washings), decarbonation with HCl and extraction after 4 h of sedimentation and preparation of the sample on glass slides. The analysis was performed on i) normal, ii) ethylene glycol saturated iii) oriented samples heated to $500 \text{ }^\circ\text{C}$. X-ray analyses of these oriented samples were performed on a CPS 120 INEL.

Pseudo-total concentrations were determined by digesting 13 air-dried soil samples (taken at various depths) in hot aqua regia. Each sample was analyzed in triplicate. The aqua regia extraction was based on the procedure recommended by the International Standardisation Organisation (ISO 11466, 1995). Samples (3 g) were placed in a 250 mL pyrex digestion tube. The pre-digestion step was first done at room temperature for 16 h with 28 mL of 37% HCl–70% HNO_3 (3:1) mixture for slow oxidation of soil organic matter. The suspension was then digested at $160 \text{ }^\circ\text{C}$ (the temperature of the reaction mixture was slowly raised) for 2 h with a reflux condenser. The suspension obtained was then filtered through an ashless Whatman filter, diluted to 100 mL with 0.5 mol L^{-1} HNO_3 and stored in polyethylene bottles for analysis. The accuracy of major and trace element assay was verified by using a certified reference material 141R (BCR, Brussels). The metal concentrations were finally measured by inductively coupled plasma optical emission spectrometry (ICP-OES) IRIS Intrepid II XDL/Thermo Electron Corporation. Samples are assayed 3 times, and the ICP gave the mean value. The same technique was also used for samples obtained from the chemical extractions described below. All concentrations are based on dry matter.

2.2. Complementary analyses

Additional analyses were performed to complete the pedological analyses. First, sequential chemical extractions were used to partially characterize the association of metals with soil components and to identify the fractions that are, or could further become, available. A 7-step sequential extraction procedure was performed, according to Leleyter and Probst (1998). Samples between 0 and 90 cm were submitted to the extraction procedure, 2 replicates for each sample. A 100 g aliquot of soil obtained by quartation was finely ground in an agate mortar and sieved through a $200 \mu\text{m}$ sieve, then 1 g of soil was submitted to the sequential extraction procedure. Each chemical fraction was operationally defined as described in Table 1. All the extractions were conducted in 120 mL Savilex beakers. The solid phase was washed with 20 mL of deionised water and dried at $45 \text{ }^\circ\text{C}$ before the next extraction step in order to prevent any dilution of reagent used in

Table 1
Protocol summary of the 7-step sequential extraction procedure (Leleyter and Probst, 1998)

Step	Fraction	Extractant	Reaction time	Temperature
1	Dissolved with water	Water (10 mL)	30 min	20 °C
2	Really exchangeable	1 M Magnesium nitrate pH 5 (10 mL)	2 h	20 °C
3	Bound to carbonates or acid-soluble fraction	1 M Sodium acetate pH 4.5 (10 mL)	5 h	20 °C
4	Bound to Mn oxides	0.1 M Hydroxylammonium chloride pH 3.5 (10 mL)	30 min	20 °C
5	Bound to amorphous iron oxides	0.2 M Ammonium oxalate+0.2 M Oxalic acid (10 mL)	4 h	20 °C
6	Bound to crystalline iron oxides	0.2 M Ammonium oxalate+0.2 M Oxalic acid+ Ascorbic acid (10 mL)	30 min	80 °C
7	Bound to organic matter or oxidizable fraction	1) 35% Hydrogen peroxide (8 mL)+0.02 M Nitric acid (3 mL) pH 2 2) 3.2 M Ammonium acetate (5 mL)	5 h	85 °C

the following step. Metal and metalloid concentrations were measured in the leachate fraction. The first step concerns the elements dissolved with water. The second aims to leach the cations adsorbed onto permanent structural charges with magnesium nitrate. A mix of sodium acetate and acetic acid in the third step leads to the dissolution of the carbonated or acid-soluble fraction. Then, analysis of the reducible fraction is divided into 3 steps. The fourth, fifth and sixth steps of the protocol progressively reduce the reducible fraction. The manganese oxides are dissolved first by hydroxylammonium chloride. Then a mixture of ammonium oxalate and oxalic acid leads to the reduction of amorphous iron oxides. In order to reach crystalline iron oxide dissolution, reduction, acid and complexation (ligand) actions were combined by addition of ascorbic acid to the previous mixture. Finally, using hydrogen peroxide, nitric acid and ammonium acetate, the last step allows the oxidation of all the oxidizable fractions.

Then, in order to observe the metals and their environments, the 0–10 cm soil horizon was studied using a Jeol LV JSM-6360 scanning electron microscope (SEM) and an energy dispersive spectrometer (EDS) for elemental analysis.

The inter-relationships between trace elements and major elements or soil characteristics (Al, Fe, Mn, Mg, pH, CEC, granulometry, carbonates, soil organic matter, $P_{\text{Joret-Hebert}}$) were performed using STATISTICA v 7.0. Only the best linear models were retained and presented. The results were then compared to sequential chemical extractions in order to identify the main phases to which metals and metalloid bind.

2.3. Study site

The method was used in an experimental site, located in the Paris basin, in the west of the Loiret (*département* No. 45), 45 km from Orleans and 80 km south of Paris. The studied soil was sampled in February 2005 near a lead-recycling plant surrounded by agricultural land with vegetable gardens located south of Bazoches-les Gallérandes along secondary road No. 927. Preliminary studies done by LARA Europe Analyses on this site showed a homogeneous distribution of lead around the plant, with decreasing concentrations as the distance from the factory increased. A pit was dug to 150 cm depth to determine the profile and the soil was sampled every 10 cm from the topsoil down to 130 cm. The very topsoil, composed of fresh grass cover, was removed. A total of 13 samples were air dried in the laboratory at 25 °C to constant weight and sieved through a 2 mm size AFNOR sieve, then homogenized and stored in paper bags.

3. Results and discussion

3.1. Pedological and physical–chemical characteristics of the soil profile (Tables 2 and 3)

The first meter of soil is mainly composed of a Quaternary loess deposit on a Tertiary marl “Marnes de Blamont”. Four horizons were mainly observed in the soil profile. The first is an A horizon from 0 to 25 cm, with a brown colour (Munsell: 7.5 YR 4/3) due to the organic matter, a very high porosity (50%) and an almost

Table 2
Physical and chemical properties of the soil profile

Depth(cm)	pH water	CEC	Sand	Silt	Clay	Carbonates	OM	P ₂ O ₅
		cmol(+) kg ⁻¹						mg kg ⁻¹
0–10	7.70±0.08	15.10±1.97	21±6.2	52.7±6.0	20.38±1.8	2.5±1.2	5.98±0.12	88±19
10–20	7.83±0.22	16.83±0.88	14.6±2.9	56.6±2.8	25.6±2.2	1.5±0.24	3.24±0.14	70±18
20–30	8.05±0.06	15.63±2.46	14.9±2.8	56.9±2.1	26.0±2.7	2.1±1.2	2.29±0.20	72±25
30–40	8.08±0.19	18.80±0.50	6.4±1.0	62.4±0.96	30.8±1.4	1.37±0.28	1.45±0.18	44±17
40–50	8.23±0.05	20.40±0.50	7.5±1.6	58.0±0.8	33.4±1.5	0.73±0.30	1.1±0.11	24±14
50–60	8.18±0.13	20.53±1.14	5.2±0.4	57.4±0.5	36.6±0.4	0.82±0.41	0.90±0.22	26±15
60–70	8.28±0.05	21.48±1.74	11.6±3.8	52.5±2.5	35.2±1.3	0.67±0.40	0.72±0.07	27±18
70–80	8.25±0.13	21.73±2.56	15.0±6.5	46.7±3.7	37.8±2.8	0.89±0.63	0.54±0.16	20±12
80–90	8.33±0.10	23.25±2.65	27.7±4.7	35.8±2.6	35.7±2.2	1.36±0.72	0.87±0.06	24±15
90–100	8.53±0.05	18.68±0.88	27.2±0.8	42.0±0.7	29.6±0.4	48.2±2.60	1.29±0.37	34±18
100–110	8.63±0.05	12.15±0.93	34.6±2.1	42.4±1.5	22.3±0.8	77.3±3.9	0.85±0.85	47±15
110–120	8.83±0.05	8.75±0.17	36.9±1.7	44.3±1.9	18.4±0.5	89.9±3.0	0.41±0.41	51±16
120–130	8.83±0.05	7.43±0.28	37.2±2.0	47.9±1.4	14.8±0.7	92.1±2.5	0.13±0.13	50±14

granular structure with a subangular polyhedral structure. The second is a cambic horizon from 25 to 90 cm, with a strong brown colour (7.5 YR 5/8) due to the presence of clay coming from phyllosilicates resulting from degradation of the loess. This horizon has a prismatic structure and its porosity decreases compared to the horizon above (15–20%). The third is a C horizon from 90 to 110 cm, it is an intermediate horizon of marl deterioration with a brownish yellow colour (10 YR 6/6). The last one is an R horizon or marl (bed rock), starting from 110 cm with a very pale brown colour (10 YR 8/3). The main soil characteristics are presented in Table 2. The calcareous soil studied presents a very alkaline pH all along the profile (pH varies from 7.2 in topsoil to 8.8 at depth). It presents very high carbonate levels at depth (93%) which quickly decrease as soon as the marl is degraded. From 85 cm to the surface, the carbonate levels remain below 2.5%.

Unlike carbonates, the proportion of clay minerals increases in the alterite horizon. Clays result from the deterioration of the silicates present in the marl and the loess and becomes very abundant in the cambic horizon (30 to 40%). About 95% of the clay minerals were recognized as illite. Illite is characterized by a basal reflection of 10 Å, unchanged after glycolation and heating to 550 °C. Then a very small amount of kaolinite was identified, characterized by a 7 Å basal reflection (in an untreated and glycolated sample) which disappears after heating (Fig. 1).

Soil organic matter (SOM) presents high concentrations in the epipedon (6%), certainly due to the presence of a lawn for nearly 60 years but perhaps also to the stabilization effect induced by the presence of large amounts of metals (Dumat et al., 2006). The SOM content generally decreased with depth, except a slight increase observed at 90 cm, that can be explained by (i) an accumulation of degraded roots which go down along the profile and remain blocked above the impenetrable calcareous horizon, (ii) dissolved organic carbon migration at high pH, or (iii) by a paleosol which is often found above the marl (BRGM, 1978).

These clay and SOM contents are associated with a cationic exchange capacity varying in the range of 7.4 to 23.2 cmol(+) kg⁻¹, following the granulometric clay profile ($r^2=0.92$). The CEC presents little variation along the whole profile. In the first 40 cm, it is explained by the strong SOM content. Then, this SOM level decreased and the CEC is explained by the high content of illite (which is a clay with a CEC between 10 and 40 cmol(+) kg⁻¹).

Available phosphorus is higher in the topsoil (88 mg P₂O₅ kg⁻¹) surely due to the contribution of phosphate-enriched fertilizers intensively added in the 70's. In depth we find high levels of phosphorus from the calcium phosphates contained in the bed rock. These phosphates are undoubtedly rather soluble and disappear during deterioration of the marl (the P₂O₅ content decreases strongly in the S horizon). High clay and phosphates could be the major bearing phases for the lead in the surface horizons. In particular, the formation of the extremely stable lead phosphates, could reduce lead availability (Diyab et al., 2003).

The soil pseudo-total calcium concentrations along the profile (Table 3) were in the range of 0.57 to 33.57% and follow the carbonate profile ($R^2=0.99$) since this soil contains calcium

carbonates. Soil pseudo-total aluminium concentrations were between 0.88 and 4.13% and follow the clay profile ($R^2=0.9$), indeed, aluminium is a component of clays which are aluminosilicates. For iron, manganese and magnesium they range between 0.52–3.29%, 0.02–0.09% and 0.30–0.56% respectively. These 3 metals follow the granulometric clay profile, but are subjected to the influence of soil organic matter in the topsoil. Indeed, below 30 cm, Fe, Mn and Mg have profiles parallel with those of clays and aluminium, because the metals are probably contained in the clays. These metals are thus well correlated with clays starting from 30 cm. Between 0 and 30 cm, they are also present in the organic matter, that is why in these first centimeters, the concentrations in Fe, Mn and Mg are explained especially by the strong content of organic matter. Nevertheless, sequential extractions showed that 71 to 93% of Fe and 62 to 79% of Mn were contained

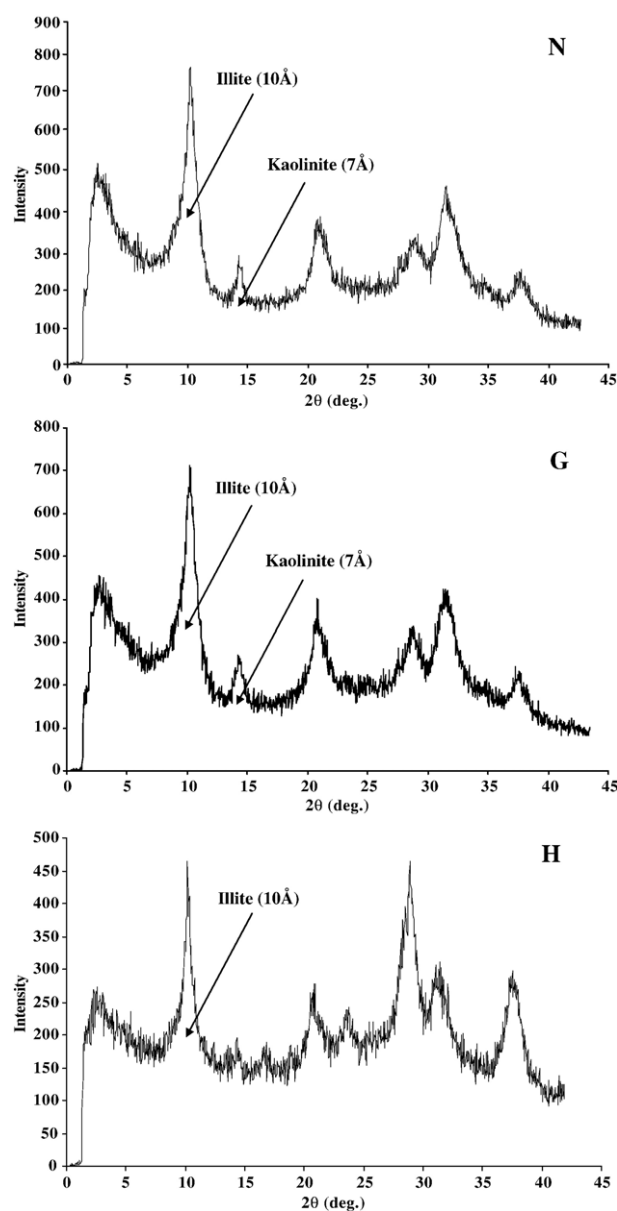


Fig. 1. X-ray diffraction pattern of the 0–10 cm horizon soil sample showing the clay minerals. (N): normal sample, (G): glycolated sample and (H): heated sample.

Table 3
Major element concentrations versus depth obtained after aqua regia digestion

Depth (cm)	(%)						
	Al	Ca	Fe	Mg	Mn	Na	P
0–10	2.64±0.08	1.22±0.02	2.31±0.06	0.39±0.01	0.07±0.001	0.29±0.025	0.06±0.001
10–20	2.65±0.02	1.14±0.01	2.45±0.19	0.37±0.01	0.07±0.002	0.08±0.014	0.05±0.001
20–30	2.65±0.05	1.05±0.01	2.46±0.03	0.37±0.00	0.07±0.001	0.05±0.013	0.05±0.001
30–40	2.84±0.09	0.95±0.01	2.40±0.04	0.40±0.02	0.07±0.002	0.04±0.008	0.03±0.001
40–50	3.04±0.03	0.65±0.01	2.65±0.04	0.44±0.00	0.06±0.001	0.03±0.002	0.03±0.001
50–60	3.13±0.03	0.57±0.01	2.73±0.07	0.45±0.01	0.06±0.001	0.03±0.001	0.03±0.001
60–70	3.37±0.07	0.63±0.01	2.96±0.06	0.48±0.01	0.06±0.001	0.03±0.001	0.02±0.000
70–80	3.68±0.07	0.68±0.01	3.18±0.06	0.52±0.01	0.07±0.001	0.03±0.001	0.02±0.000
80–90	4.13±0.08	1.09±0.02	3.29±0.07	0.56±0.01	0.09±0.002	0.04±0.001	0.03±0.001
90–100	2.28±0.05	18.21±0.36	1.77±0.04	0.37±0.01	0.05±0.001	0.04±0.001	0.02±0.000
100–110	1.35±0.03	28.84±0.58	0.99±0.02	0.31±0.01	0.03±0.001	0.04±0.001	0.02±0.000
110–120	0.92±0.02	33.22±0.66	0.58±0.01	0.30±0.01	0.02±0.000	0.04±0.001	0.01±0.000
120–130	0.88±0.02	33.57±0.67	0.52±0.01	0.31±0.01	0.02±0.000	0.05±0.001	0.01±0.000

in the 3 reducible fractions (steps 4, 5 and 6), which means that these metals are mainly in the form of oxide in this soil.

3.2. Solum trace element pattern

The pseudo-total concentrations of trace elements obtained from aqua regia digestion, versus depth are given in Table 4. Two different behaviors for these trace elements in soils can be observed.

First, Ni and Cr levels were 7.5–41 mg kg⁻¹ and 14.5–92.7 mg kg⁻¹ respectively. These concentrations increased with depth along the profile to reach maximum values in the C horizon and are close to those found in the lithosphere. Indeed, according to Baize (2002) mean natural concentrations are around 50 mg kg⁻¹ for Cr and 40 mg kg⁻¹ for Ni.

By contrast, Pb, As, Cu, Sb, Sn and Zn peak in the upper part of the profile, and are significantly higher than in the R horizon. Lead concentration in the topsoil was 1932 mg kg⁻¹ and decreased rapidly with depth. Indeed, this concentration is already divided by 2.5 in the next sample (785 mg kg⁻¹ in the 10–20 cm horizon). From 50–60 cm, concentrations were low (around 40 mg kg⁻¹) and remained almost constant before reaching the

marl. These concentrations are close to the background level, according to the work of Baize (2002) in a study in the same region. Indeed, he reports that in the limestone of the Beauce area, the common pedogeochemical background level of lead is estimated at 40 mg kg⁻¹, as found in the current work at 60 cm.

In the same way, Sb and Sn varied between 0 and 67.4 mg kg⁻¹ and 1.1 to 36.8 mg kg⁻¹ respectively from depth to the surface. These concentrations largely exceed the natural surface concentrations for these 2 metals. For Sb, background levels are between 0.2 and 10 mg kg⁻¹ (Baize, 2002). Moreover, a soil is considered as polluted starting from 30 mg kg⁻¹. For Sn, the natural content of the uncontaminated soil is approximately 5 mg kg⁻¹ (Kabata-Pendias and Pendias, 1992).

Finally, the profiles of As, Cu, and Zn are close to that of Pb, Sb and Sn, but at lower concentrations. Arsenic concentrations varied from 3 mg kg⁻¹ at depth to 28 mg kg⁻¹ in the topsoil which indicates contamination. Indeed, according to Alloway (1995), an unpolluted soil contains between 1 and 20 mg kg⁻¹. For Cu, concentrations ranged from 4 to 34 mg kg⁻¹ whereas those found in the tilled horizons of this area of Calcaires de Beauce lie between 11 and 20 mg kg⁻¹ (Baize, 2002). For Zn, concentrations ranged

Table 4
Trace element concentrations versus depth obtained after aqua regia digestion

Depth (cm)	mg kg ⁻¹							
	As	Cr	Cu	Ni	Pb	Sb	Sn	Zn
0–10	28.08±2.20	61.83±1.03	34.23±0.54	33.36±1.75	1932.58±7.40	67.38±1.35	36.84±0.74	86.90±2.69
10–20	19.48±0.39	65.46±0.29	20.43±0.95	28.66±1.22	785.02±1.54	34.14±0.68	17.19±0.34	68.28±0.70
20–30	13.66±0.91	64.97±2.33	13.58±0.92	30.40±6.28	279.88±8.19	11.16±0.22	10.55±0.21	70.77±5.53
30–40	11.50±0.00	69.77±1.66	10.58±0.26	26.08±1.98	139.48±8.29	4.36±0.09	3.03±0.06	61.78±16.66
40–50	11.32±0.19	74.88±0.80	9.10±0.06	27.08±0.97	83.40±1.46	2.30±0.05	1.89±0.04	52.39±0.75
50–60	12.25±0.19	81.23±0.61	8.65±0.02	29.35±1.13	56.26±0.78	0.93±0.02	1.90±0.04	54.81±0.92
60–70	12.23±0.24	83.24±1.66	8.41±0.17	30.86±0.62	44.89±0.90	0.40±0.01	1.44±0.03	55.23±1.10
70–80	13.74±0.27	90.51±1.81	8.61±0.17	35.84±0.72	31.83±0.64	0.00±0.00	1.54±0.03	61.38±1.23
80–90	15.26±0.31	92.67±1.85	9.42±0.19	40.79±0.82	41.79±0.84	0.39±0.01	1.10±0.02	61.64±1.23
90–100	10.02±0.20	48.49±0.97	6.51±0.13	20.40±0.41	35.60±0.71	0.87±0.02	1.81±0.04	30.49±0.61
100–110	5.34±0.11	26.83±0.54	4.36±0.09	12.22±0.24	23.48±0.47	0.83±0.02	4.77±0.10	16.46±0.33
110–120	3.33±0.07	15.92±0.32	3.75±0.07	7.43±0.15	3.63±0.07	0.00±0.00	1.43±0.03	8.57±0.17
120–130	3.01±0.06	14.54±0.29	3.94±0.08	8.04±0.16	3.59±0.07	0.11±0.00	1.65±0.03	7.96±0.16

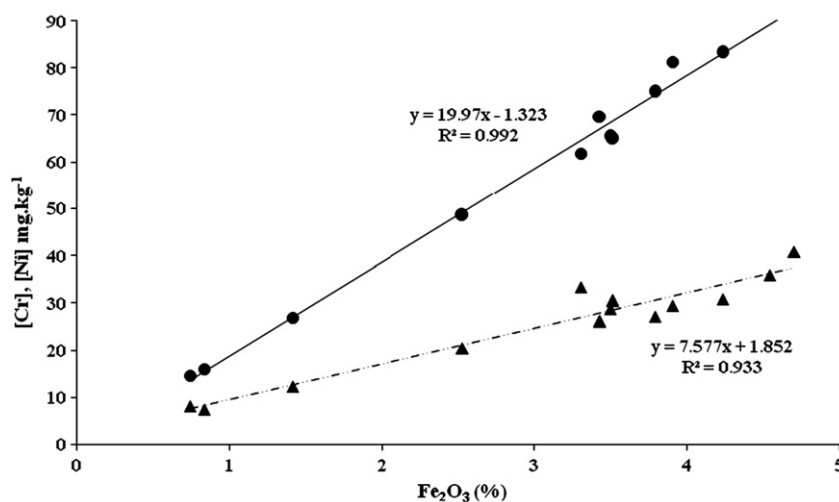


Fig. 2. Correlation between soil pseudo-total Fe₂O₃ and Cr (●) or Ni (▲) concentrations.

from 8 to 87 mg kg⁻¹: those at the pedogeochemical bottom background of the agricultural soils of the plain of Beauce do not exceed 80 mg kg⁻¹ according to the same author.

The patterns of these trace elements in the solum indicate that the soil is contaminated by Pb, As, Cu, Sb, Sn and Zn in the upper horizons. Thus, we can note a very strong anthropogenic contribution for Pb, Sb and Sn. Concerning As, Cu and Zn, contamination exists, but is less marked. Indeed, during the process, lead-acid batteries are melted down and refined to purify the lead residue obtained. During this phase, several metals are eliminated including As, Cu, Sb and Sn. In fact, Zn is currently added during refining. This explains why, in addition to lead contamination, the soil contains abnormally high As, Cu, Zn, Sb and Sn levels.

3.3. Relations between trace metals and metalloids versus major elements

Studying the correlations between the soil characteristics and all the parameters presented in Tables 1 and 2, iron was the element which best explains the distribution of metals and the metalloid along the soil profile. Such high affinity between iron and trace metals has been shown in previous pedological studies. Sparks (1995) proposed selectivity sequences for the adsorption or coprecipitation of divalent metal cations on various hydrous iron oxides. Gavalda (2001) and Cornu et al. (2005) found that iron oxides were between 2- and 17-fold more concentrated in trace metals than in bulk non-contaminated soils. Our results confirm that the relationship between iron oxides and trace elements can be used to detect anomalies in trace element patterns. These relations enabled us to distinguish 2 groups of metals. One group concerns elements for which concentrations obey the same laws all along the profile. Such elements were assumed not to present concentration anomalies. Another group concerns metals for which the relationships with major elements are strongly perturbed as we approach the surface. These elements were assumed to be enriched by the plant fallout.

3.3.1. Constant relation with iron along the profile: nickel and chromium

Among major elements, iron is the most correlated to nickel and chromium. Indeed, linear regression analysis was performed between Ni and Cr versus Fe (Fig. 2). Results showed that Ni and Cr are very well delineated by iron oxides, with a constant relationship all along the profile ($r^2=0.99$ for Cr with $n=13$ and $p<0.001$ and 0.93 for Ni with $n=13$ and $p<0.001$). Such a good linear correlation suggests a high affinity of Ni and Cr for Fe. These results are confirmed by sequential extractions performed on the soil samples. Indeed, they showed that 71–89% of Cr and 51–81% of Ni are contained in the 3 reducible fractions (steps 4, 5 and 6). Data from linear regression analysis and sequential extractions combined with pseudo-total concentrations confirmed that these elements are mainly derived from soil minerals, without the impact of industrial atmospheric input. Moreover, Cr and Ni results were strongly correlated confirming their common natural origin ($r^2=0.9$; $p<0.001$; $n=13$).

3.3.2. Relation with iron perturbed in surface

3.3.2.1. Lead. As already shown by other studies on contaminated soils (Ge et al., 2000; Dumat et al., 2001; Ettler et al., 2005; Dumat et al., 2001, 2006), our results highlight a high lead concentration in the topsoil, decreasing quickly with depth as seen in Fig. 3.

Linear regression analysis performed between pseudo-total (aqua regia) [Pb] (mg kg⁻¹) and [Fe₂O₃] (%) showed that, below 60 cm depth, lead is mainly bound to iron oxides with the following equation:

$$[\text{Pb}] = 9.4883 \times [\text{Fe}_2\text{O}_3] + 2.9787 \quad (r^2 = 0.7141; n = 7; p = 0.0083) \quad (1)$$

These results combined with the pseudo-total concentrations at 60 cm depth (around 40 mg kg⁻¹) indicate that the background level is reached at this depth. In order to check that the unpolluted level was reached, relationships between Pb and Fe assessed on

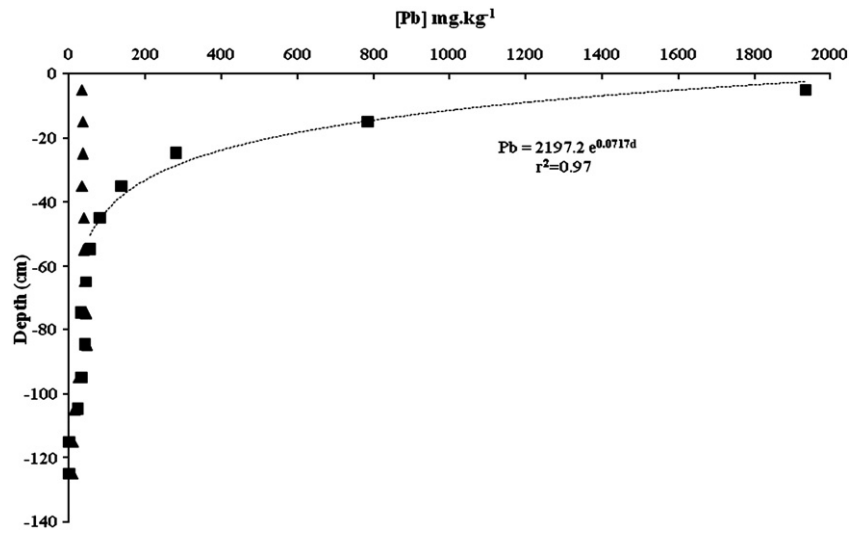


Fig. 3. Comparison between the soil pseudo-total lead concentrations obtained after aqua regia digestion (■) and those predicted by the linear regression analysis between Pb and Fe₂O₃ starting from 60 cm (Eq. (1)) (▲).

various solums by several authors (Gavalda, 2001; Navas and Machin, 2002; Velde et al., 2003; Tyler, 2004; Sipos et al., 2005; Lamy et al., 2006) were compared to our results (Fig. 4). All their data were collected in soil profiles without any point source pollution. In all cases, the Pb–Fe relationship was very close to the data we collected in our profile below 60 cm. This led us to conclude that below this depth contamination was negligible.

Thus, in the soil studied, anthropogenic lead resulting from the plant's activity seems to have migrated down to 60 cm, below this depth, the background concentration is reached. The plant being in activity since 1967, lead crossed approximately 60 cm in 40 years. The speed of migration of lead can therefore be estimated at 1.5 cm per year. The equation obtained during

the analysis by linear regression between the lead and the iron oxides below 60 cm was used to predict the concentrations on the surface in the absence of anthropogenic contamination. The results reported in Fig. 3 clearly show that the concentrations actually obtained diverge strongly from those extrapolated from the values at 60 cm, indicating contamination at this depth.

In the first 60 cm, the Pb concentrations were 2–40-fold higher than the natural background, and largely exceeding the critical soil concentrations defined by Kabata-Pendias and Pendias (1992). Indeed, they consider that above 400 mg kg⁻¹ Pb in a soil, toxicity is possible. Thus, in this soil, the strong anthropogenic contamination and the possible vertical mobility of Pb along the profile may be considered. Linear regression analysis performed

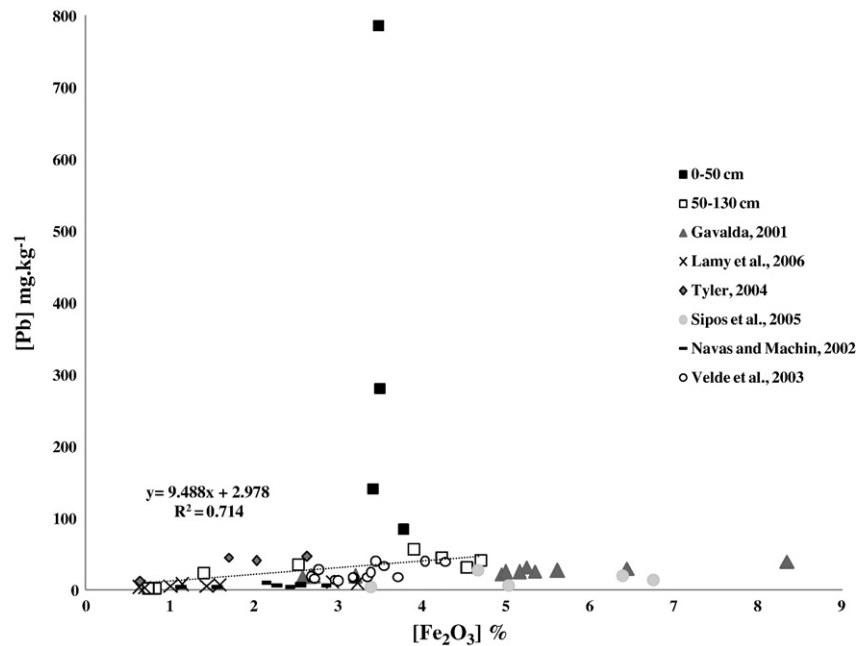


Fig. 4. Correlations between soil pseudo-total Pb and iron oxide Fe₂O₃ concentrations between 0 and 50 cm (■) or 50 and 130 cm (□), compared with data collected on uncontaminated soils.

in the first 60 cm, indicated that anthropogenic lead is strongly influenced by soil organic matter ($r^2=0.96$). These results are in agreement with those obtained in a similar context of industrial contamination by Dumat et al. (2001, 2006) and Diyab et al. (2003).

The topsoil clearly contained elevated levels of lead, the sequential extractions gave an indication of its distribution in various soil pools and of their potential for mobilization into the aqueous phase. The chemical extraction results are summarized in Table 5. Between 0 and 50 cm lead is mainly found in the acid-soluble fraction (step 3) over a range of 40 to 60%. Therefore, we can estimate that lead is mainly bound to carbonates and phosphates because the sodium acetate treatment can dissolve both these compounds. In the first 50 cm, the remainder of the lead was contained mainly in the iron oxides (steps 5 and 6) (20–50%) and then in organic matter (step 7). Although direct comparison is not possible because of the different extraction methods used, this is in apparent agreement with a study by Clemente et al. (2006), in calcareous soil from a former Pb–Zn mine area heavily contaminated by lead (1572 mg kg^{-1}), indeed, they found 42% of the lead in the same acid-soluble fraction. In a study by Kabala and Singh (2001), the surface horizon of a highly contaminated soil was found to contain up to 45% carbonate-bound Pb. The geochemical Pb^{2+} characteristics allow lead to bind to carbonates in calcareous soils where the metals are precipitated or coprecipitated depending on pH (Dang et al., 2002). In addition, as shown in this work, Kabata-Pendias and Pendias (1992) and Dumat et al. (2001) found accumulation of lead in the organic fraction with relatively strong interactions. It is interpreted as the amount of metal that can be released in strong oxidizing conditions due to organic matter degradation (Tessier et al., 1979; Dumat et al., 1997; Ettler et al., 2005).

Then between 50 and 90 cm, the lead behavior differed, confirming the linear regression analysis. Indeed, lead was mainly found in the 3 reducible fractions (steps 4, 5, 6) (39 to 76%) and the remainder was divided between the acid-soluble and oxidizable fractions. Many authors have shown that lead has a preference for manganese or iron oxides. Indeed, according to Tessier et al. (1979), Dang et al. (2002) and Banat et al. (2005), Fe and Mn oxides are excellent scavengers for trace metals and they can be mobilized under reducing and acid conditions.

Thus, in our study, the oxide occluded fraction of Pb is not the dominant fraction in the contaminated horizons contrary to what has been reported by several authors (Ramos et al., 1994; Ahumada et al., 1999). This distribution suggests that there are insufficient iron oxides in the soil to bind all the lead or that the interaction between oxides and the other soil components (soil organic matter in particular) could modify their affinity for metals (Cheshire et al., 2000). Lead is then fixed on carbonates, which are present all along the soil profile at a constant value (around 2%) in the 90 first centimeters.

The water and $\text{Mg}(\text{NO}_3)_2$ exchangeable extractions (steps 1 and 2) performed on the topsoil (0–10 cm horizon) represent a very small percentage (0.3%), meaning that the epipedon contains 4.2 mg kg^{-1} in these fractions. They are considered to be the most mobile and available phase present in the soil (Tessier et al., 1979; Banat et al., 2005). This underlines a potential risk of transfer into the trophic chain or toxicity to living organisms. These results are in agreement with the findings of other studies. Indeed Elless et al. (2007) found that in urban yards, exchangeable lead represented 0.3% of the total lead concentration, concluding that the lead remaining in the soil is strongly sorbed to the soil or exists in largely insoluble forms. Clemente et al. (2006), found that the lead concentration in soil solution never exceeded 0.5 mg kg^{-1} .

3.3.2.2. *Arsenic, copper, zinc, antimony and tin.* As, Cu and Zn have a behavior close to that of lead, with abnormal concentrations in the first centimetres. But we demonstrate that they occurred at lower concentrations.

Linear regression analysis performed between As, Cu and Zn and iron oxides showed a good correlation for these 3 metals with iron oxides, but only starting from 40 cm (as shown in Eqs. (2) (3) (4)). The relationship governing the levels of pseudo-total [Cu] (mg kg^{-1}) and $[\text{Fe}_2\text{O}_3]$ (%) between 40 and 130 cm is the following:

$$[\text{Cu}] = 1.439 \times [\text{Fe}_2\text{O}_3] + 2.707 \quad (r^2 = 0.96; n = 9; p < 0.001) \quad (2)$$

This model is very close to that found by Lamy et al. (2006) in a deep unpolluted horizon of a Luvisol.

Table 5
Distribution of lead in each fraction of the sequential extraction procedure with Step 1: extractible with H_2O ; Step 2: exchangeable; Step 3: acid-soluble fraction; Step 4: bound to manganese oxides; Step 5: bound to amorphous iron oxides; Step 6: bound to crystalline iron oxides and Step 7: oxidizable fraction

	[Pb] mg kg^{-1} soil									
	Depth (cm)									
	0–10	10–20	20–30	30–40	40–50	50–60	60–70	70–80	80–90	
1	1.10±0.28	0.16±0.15	0.00±0.00	0.01±0.02	0.01±0.020	0.01±0.003	0.00±0.00	0.08±0.02	0.01±0.004	
2	3.08±0.98	0.25±0.30	0.00±0.00	0.06±0.12	0.00±0.00	0.00±0.00	0.00±0.00	0.00±0.00	0.00±0.00	
3	963.81±36.48	341.52±24.30	96.89±4.31	48.02±1.18	30.68±1.365	12.55±0.56	4.59±0.20	8.23±0.37	9.10±0.41	
4	6.09±1.66	2.80±0.32	1.24±0.005	0.40±0.04	0.28±0.004	0.20±0.03	0.22±0.04	0.14±0.02	0.13±0.02	
5	173.33±44.61	94.25±0.69	47.57±6.42	25.97±3.66	34.69±4.683	18.52±2.50	16.76±2.26	12.36±1.67	6.39±0.86	
6	139.00±6.72	75.67±3.57	35.67±2.14	19.58±1.61	10.55±0.633	7.47±0.45	6.61±0.40	5.61±0.34	6.10±0.37	
7	370.48±4.53	147.69±18.87	58.85±2.94	25.37±0.04	2.82±0.141	3.50±0.17	2.85±0.14	1.84±0.09	11.02±0.55	
∑ fractions	1656.89	662.34	240.23	119.41	79.03	42.25	31.03	28.26	32.77	
<i>Aqua regia</i>	1932.58	785.02	279.88	139.48	83.40	56.26	44.89	31.83	41.79	

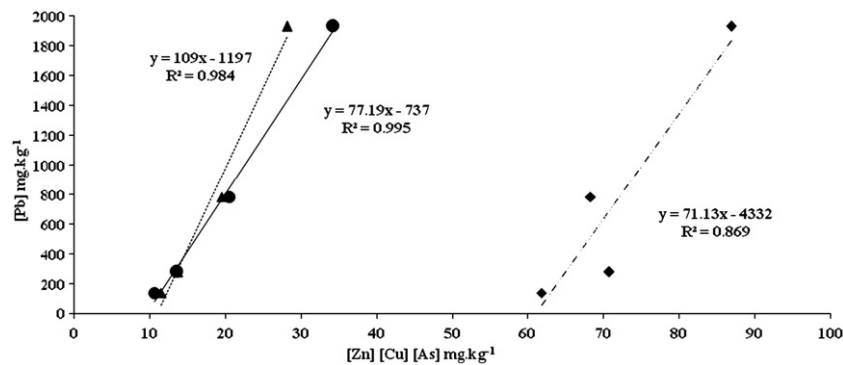


Fig. 5. Correlation between soil pseudo-total lead and As (▲) or Cu (●) or Zn (◆) concentrations in the first 40 cm.

For arsenic and zinc the following relationships are obtained (between pseudo-total [As] mg kg^{-1} and $[\text{Fe}_2\text{O}_3]$ (%) and pseudo-total [Zn] mg kg^{-1} and $[\text{Fe}_2\text{O}_3]$ (%)):

$$[\text{As}] = 2.7961 \times [\text{Fe}_2\text{O}_3] + 1.3193 \quad (r^2 = 0.971; n = 9; p < 0.001) \quad (3)$$

$$[\text{Zn}] = 14.147 \times [\text{Fe}_2\text{O}_3] - 3.1793 \quad (r^2 = 0.99; n = 9; p < 0.001) \quad (4)$$

Concentrations in the samples between 0 and 40 cm did not follow these models. This indicates anthropogenic contamination of the first 40 cm, in agreement with the concentration anomalies at the surface described above. However, this contamination is much less marked than that observed for lead.

Sequential extraction results confirmed the regression analysis. Indeed, 86–90% As, 47–87% Cu and 66–82% Zn are contained in the 3 reducible fractions, indicating that even if there is As, Cu and Zn contamination, iron and manganese oxides contain sufficient sites to retain these metals. Similar distributions have been reported in previous studies (Ramos et al., 1994; Ahumada et al., 1999; Maiz et al., 2000).

Sb and Sn present the same profile as lead: high concentrations in topsoil, which decrease with the depth. Indeed, unlike As, Cu and Zn, concentrations for Sb and Sn are much higher than normally found in the natural background. This is particularly

problematic for Sb, which is considered by the US EPA (1979) with lead and arsenic as one of the priority pollutants. Linear regression analysis performed for these 2 metals, did not allow identification of the major bearing phase.

3.4. Modelling multi-metallic contamination

The metallic contamination can be firstly modeled according to depth. Sb, Sn, Cu, Zn, As and Pb pseudo-total concentrations (mg kg^{-1}) are maximum in the topsoil and decrease strongly with depth in the upper part of the profile following exponential models (Fig. 3) as below where z is the depth in centimeters:

$$[\text{Pb}] = 2197 e^{-0.0717 z} \quad r^2 = 0.971 \quad (\text{from } 0 \text{ to } 60 \text{ cm depth})$$

$$[\text{Sb}] = 107 e^{-0.0871 z} \quad r^2 = 0.995 \quad (\text{from } 0 \text{ to } 60 \text{ cm depth})$$

$$[\text{Zn}] = 86.95 e^{-0.0099 z} \quad r^2 = 0.791 \quad (\text{from } 0 \text{ to } 40 \text{ cm depth})$$

$$[\text{Sn}] = 56 e^{-0.0768 z} \quad r^2 = 0.980 \quad (\text{from } 0 \text{ to } 50 \text{ cm depth})$$

$$[\text{Cu}] = 39 e^{-0.0393 z} \quad r^2 = 0.977 \quad (\text{from } 0 \text{ to } 40 \text{ cm depth})$$

$$[\text{As}] = 35.6 e^{-0.036 z} \quad r^2 = 0.999 \quad (\text{from } 0 \text{ to } 30 \text{ cm depth})$$

In all these equations, the first coefficients indicate the absolute value of metallic contamination in the epipedon (for $z=0$). It was maximum for Pb and decreased for the next elements in the following order $\text{Pb} > \text{Sb} > \text{Zn} > \text{Sn} > \text{Cu} > \text{As}$. Furthermore, the exponential coefficient indicated the contamination relative to natural content in the deep horizon giving another order $\text{Sb} > \text{Sn} > \text{Pb} > \text{Cu} > \text{As} > \text{Zn}$. While regression was calculated for Pb and Sb over

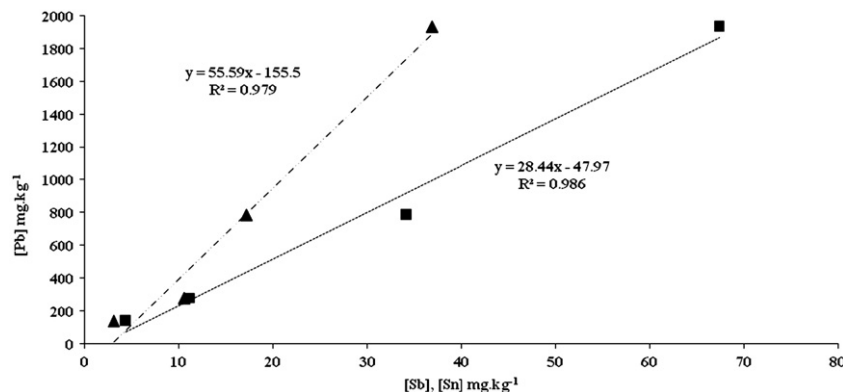


Fig. 6. Correlation between soil pseudo-total lead and Sb (■) or Sn (▲) in the first 40 cm.

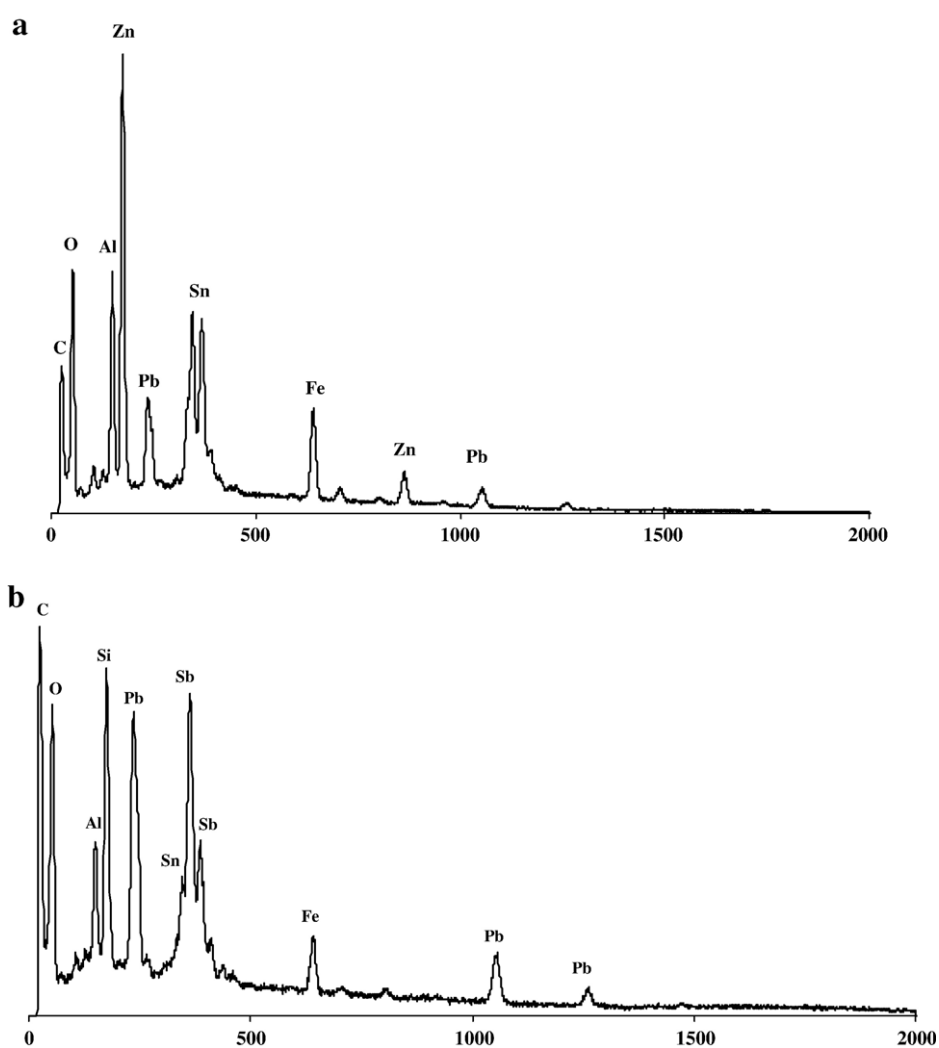


Fig. 7. SEM-EDS observation for the surface soil.

0–60 cm depth, it was only down to 50 cm for Sn, 40 cm for Zn and Cu and 30 cm for As. Consequently, Pb and Sb have moved further down the profile than Sn, which has moved more than Zn, Cu and finally As. The affinity of soil organic matter for lead and the possible migration of lead in organic colloids could be mechanisms enhancing lead mobility along the profile according to Semlali (2000).

Secondly, the interrelationship between metals gives additional simple models (Figs. 5 and 6) to describe anthropogenic contamination: in this case metal-enriched atmospheric fallout (Pb, As, Cu, Zn, Sb and Sn) from the plant. Linear correlations between Pb and the other metals were observed. This confirms the hypothesis of multi-element contamination due to the plant's activity. This information is confirmed by SEM-EDS observation of the soil surface sample, most affected by the plant's activity. Indeed, it shows that among the 50 observation points, in more than 50% of the cases, lead was associated with Sb and Sn (Fig. 7). We also found Pb–Zn or Pb–Cu associations but which were much rarer only representing about 10% of the associations. Lead also exists in aggregates containing of iron and manganese. In spite of the phosphorus content, no Pb–P associations were found by such observations.

4. Conclusions and perspectives

In regard to association with major elements, the trace elements did not have the same pattern along the profile. Ni and Cr showed a constant linear relation versus Fe along the profile indicating that their common origin is explained by geochemistry. On the contrary, Pb, Sb, Sn, As, Cu, and Zn did not obey the same model from the topsoil to the marl. Finally, the global pedological approach used in this study indicates that this industrial area has been severely affected by the activity of the lead-recycling plant, leading to accumulations of multi-metallic contamination. Indeed, high Pb, Sb and Sn concentrations and, to a lesser extent, As, Cu, and Zn have been noted in the surface soil compared with background levels.

In particular, lead is mainly accumulated in the surface soil horizon due to its relatively low mobility and strong association to soil constituents. However, results of pseudo-total concentration combined with linear regression analysis showed that the anthropogenic lead migrated down to 60 cm, at 1.5 cm per year. Sb migrated with the same speed, while Sn moved a little slower, then Cu, Zn and finally As. Moreover, depending on the soil composition and the presence or absence of anthropogenic

lead, the proportions of metals contained in the sequential extraction fractions can change. Indeed, in the uncontaminated deep horizons, the main lead carriers were iron oxides, while in the contaminated levels they were carbonates. This phenomenon illustrates the importance of studies using real contaminated soils and not simply artificially contaminated soils.

Moreover, sequential extraction performed on the 0–10 cm soil sample showed that the water-soluble fraction contained 1.1 mg Pb kg⁻¹ and the exchangeable fraction contained 3.1 mg Pb kg⁻¹. Therefore, the topsoil horizon contains 4.2 mg kg⁻¹ lead which is easily mobilisable and available. This underlines the existence of a potential risk of lead transfer to the biosphere. The ecological threat of lead is mainly associated with its mobility in the soil system which is controlled by its speciation and compartmentalization.

Acknowledgements

This work was supported by MENRT. The authors are very grateful to Thierry Aigouy for his participation in the SEM-EDS observations.

References

- Ahamed, M., Siddiqui, M.K.J., 2007. Low level lead exposure and oxidative stress: current opinions. *Clinica Chimica Acta* 383, 57–64.
- Ahumada, I., Mendoza, J., Ascar, L., 1999. Sequential extraction of heavy metals in soils irrigated with wastewater. *Communications in Soil Science and Plant Analysis* 30, 1507–1519.
- Alkorta, I., Hernandez-Allica, J., Becerril, J.M., Amezcaga, I., Albizu, I., Garbizu, C., 2004. Recent findings of the remediation of soil contaminated with environmentally toxic heavy metals and metalloids such as zinc, cadmium, lead and arsenic. *Review in Environmental Science and Bio/Technology* 3, 71–90.
- Alloway, B.J., 1995. Heavy metals in soils, 2nd edition. Blackie Academic & Professional, London.
- Bacon, J.R., Farmer, J.G., Dunn, S.M., Graham, M.C., Vinogradoff, S.I., 2006. Sequential extraction combined with isotope analysis as a tool for the investigation of lead mobilisation in soils: application to organic-rich soils in an upland catchment in Scotland. *Environmental Pollution* 141, 469–481.
- Baize, D., 2002. Les éléments traces métalliques dans les sols, INRA éditions.
- Banat, K.M., Howari, F.M., Al-Hamad, A.A., 2005. Heavy metals in urban soils of central Jordan: should we worry about their environmental risks? *Environmental Research* 97, 258–273.
- BRGM, 1978. Carte géologique de la France à 1/50000. Neuville-Aux-Bois. N°327. Ministère de l'industrie, du commerce et de l'artisanat. Service géologique national. Bureau de recherches géologiques et minières, Orléans, France. BP 6009.
- Cheshire, M.V., Dumat, C., Fraser, A.R., Hillier, S.J., Staunton, S., 2000. The interaction between soil organic matter and soil clay minerals by selective removal and controlled addition of organic matter. *European Journal of Soil Science* 51, 497–509.
- Chirenje, T., Ma, L.Q., Reeves, M., Szulczewski, M., 2004. Lead distribution in near-surface soils of two Florida cities: Gainesville and Miami. *Geoderma* 119, 113–120.
- Clemente, R., Escolar, A., Bernal, M.P., 2006. Heavy metal fractionation and organic matter mineralisation in contaminated calcareous soil amended with organic materials. *Bioresource Technology* 97, 1894–1901.
- Cornu, S., Deschattrettes, V., Salvador-Blanes, S., Clozel, B., Hardy, M., Branchut, S., Le Forestier, L., 2005. Trace element accumulation in Mn–Fe-oxide nodules of a planosolic horizon. *Geoderma* 125, 211–224.
- Dang, Z., Liu, C., Haigh, M., 2002. Mobility of heavy metals associated with the natural weathering of coal mine spoils. *Environmental Pollution* 118, 419–426.
- Diyab, C., Juillot, F., Dumat, C., 2003. Study of Pb phosphates in the rhizosphere soils of various plants by chemical and physical technics. *International Conference on Metals in the Environment*, Grenoble.
- Dumat, C., Cheshire, M.V., Fraser, A., Shand, C., Staunton, S., 1997. The effect of removal of soil organic matter and iron on the adsorption of radiocaesium. *European Journal of Soil Science* 48, 675–683.
- Dumat, C., Chiquet, A., Gooddy, D., Aubry, E., Morin, G., Juillot, F., Benedetti, M.F., 2001. Metal ion geochemistry in smelter-impacted soils and soil solutions. *Bulletin de la Société Géologique de France* 172, 539–548.
- Dumat, C., Quenea, K., Bermond, A., Toinen, S., Benedetti, M.F., 2006. A study of the trace metal ion influence on the turn-over of soil organic matter in various cultivated contaminated soils. *Environmental Pollution* 142, 521–529.
- Elless, M.P., Bray, C.A., Blaylock, M.J., 2007. Chemical behavior of residential lead in urban yards in the United States. *Environmental Pollution* 148, 291–300.
- Ettler, V., Vanek, A., Mihajevic, M., Bezdzicka, P., 2005. Contrasting lead speciation in forest and tilled soils heavily polluted by lead metallurgy. *Chemosphere* 58, 1449–1459.
- FAO, 1998. World reference base for soil research. *World Soil Resources Report*, vol. 84. FAO, Rome.
- Gavaldà, D., 2001. Devenir des éléments traces métalliques dans les brouillards (luvi-redoxisol) après épandage de boues granulées. Thèse de doctorat, INP-ENSAT. 258 pp.
- Ge, Y., Murray, P., Hendershot, W.H., 2000. Trace metal speciation and bio-availability in urban soils. *Environmental Pollution* 107, 137–144.
- Han, F.X., Banin, A., Kingery, W.L., Triplett, G.B., Zhou, L.X., Zheng, S.J., Ding, W.X., 2003. New approach to studies of heavy metal redistribution in soil. *Advances in Environmental Research* 8, 113–120.
- Ho, M.D., Evans, G.D., 2000. Sequential extraction of metal contaminated soil with radiochemical assessment of readsorption effects. *Environmental Science and Technology* 34, 1030–1035.
- ISO 11466, 1995. Soil quality. Extraction of trace elements soluble in aqua regia. International Organization for Standardisation, Geneva, Switzerland.
- Kabala, C., Singh, B.R., 2001. Fractionation and mobility of copper, lead and zinc in soil profiles in the vicinity of a copper smelter. *Journal of Environmental Quality* 30, 485–492.
- Kabata-Pendias, A., Pendias, H., 1992. Trace elements in soils and plants, 2nd edition. CRC press, Boca Raton, FL.
- Lamy, I., Van Oort, F., Dere, C., Baize, D., 2006. Use of major- and trace-element correlations to assess metal migration in a sandy Luvisol irrigated with waste water. *European Journal of Soil Science* 57, 731–740.
- Leleyter, L., Probst, J.L., 1998. A new sequential extraction for the speciation of particulate trace elements in river sediments. *International Journal of Environmental Analytical Chemistry* 73, 109–128.
- Maiz, I., Arambarri, I., Garcia, R., Millán, E., 2000. Evaluation of heavy metal availability in polluted soils by two sequential extraction procedures using factor analysis. *Environmental Pollution* 110, 3–9.
- Navas, A., Machin, J., 2002. Spatial distribution of heavy metals and arsenic in soils of Aragon (northeast Spain): controlling factors and environmental implications. *Applied Geochemistry* 17, 961–973.
- Quevauviller, P., Vand Der Sloot, H.A., Muntau, H., Gomez, A., Rauret, G., 1996. Conclusion of the workshop: harmonization of leaching/extraction tests for environmental risk assessment. *Science of the Total Environment* 178, 133–139.
- Raksasataya, M., Langdon, A.G., Kim, N.D., 1996. Assessment of the extent of lead redistribution during sequential extraction by two different methods. *Analytica Chimica Acta* 332, 1–14.
- Ramos, L., Hernandez, L.M., Gonzales, M.J., 1994. Sequential fractionation of copper, lead, cadmium and zinc in soils from Donana National park. *Journal of Environmental Quality* 23, 50–57.
- Schramel, O., Michalke, B., Ketrup, A., 2000. Study of the copper distribution in contaminated soils of hop fields by single and sequential extraction procedures. *Science of the Total Environment* 263, 11–22.
- Semlali, R., 2000. Localisation, dynamique et estimation de flux d'éléments traces métalliques dans les sols. PhD ENGREF, Paris, France. 112 pp.
- Sipos, P., Nemeth, T., Mohai, I., Dodony, I., 2005. Effect of soil composition on adsorption of lead as reflected by a study on a natural forest soil profile. *Geoderma* 2005, 363–374.
- Sparks, D.L., 1995. *Environmental soil chemistry*. Academic Press, New-York.

- Tessier, A., Campbell, P.G.C., Bisson, M., 1979. Sequential extraction procedure for the speciation of particulate trace metals. *Analytical Chemistry* 51, 844–851.
- Tyler, G., 2004. Vertical distribution of major, minor, and rare elements in Haplic Podzol. *Geoderma* 119, 277–290.
- Ure, A.M., Davidson, C.M., Thomas, R.P., 1995. Single and sequential extraction schemes for trace metal speciation in soils and sediments. In: Quevauviller, P., Maier, E.A., Griepink, B. (Eds.), *Quality Assurance for environmental analysis (BCR)*. Elsevier, pp. 505–523.
- US EPA, 1979. Water related fate of the 129 priority pollutants EP-440/4-79-029A. Washington DC., vol. 1.
- US EPA, 2001. Identification of dangerous levels of lead: final rule. *Federal Register* 66 (4), 1205–1240 January 5.
- Velde, B., Church, T., Bauer, A., 2003. Contrasting trace element geochemistry in two American and French salt marshes. *Marine Chemistry* 83, 131–144.